DNA Electrophoresis

DOI: 10.1002/anie.200906343

DNA Dynamics in Nanoscale Confinement under Asymmetric Pulsed Field Electrophoresis**

*Neda Nazemifard, Subir Bhattacharjee, Jacob H. Masliyah, and D. Jed Harrison**

The difficulty of fabricating tight nanoscale confinements has limited the understanding of DNA dynamics inside structures with pores smaller than the persistence length (≈ 50 nm) of DNA molecules.[1–3] Our group has developed colloidal self-assembly (CSA) of crystalline arrays of particles within microfluidic channels as a powerful tool for the easy fabrication of ordered nanoporous media.[4] Angular separation of DNA has been achieved using asymmetric pulsed field electrophoresis within such crystalline arrays.[5] Here, nanoparticle arrays with particles as small as 100 nm (corresponding to ca. 15 nm pore sizes) were successfully fabricated, and the mechanism of DNA transport in highly confined pores was studied.

DNA separation was conducted using a microfluidic chip filled with an array of nanoparticles as a sieving matrix. A schematic of the PDMS microchip is shown in Figure 1 a. Aqueous suspensions of monodisperse silica colloids (Bangs Laboratories, Fishers, IN) of 100, 330, and 700 nm diameter were used to form self-assembled nanoparticle arrays inside the microchips.[4,5] SEM images of the self-assembled structure reveal a closely packed hexagonal array of nanoparticles, where the size of pores (the smallest opening between the particles, d_p) were around 15% of the particle size, i.e., $d_p =$ 15, 50, and 105 nm for 100, 330, and 700 nm particles, respectively. Angular separation of DNA molecules under a pulsed field was achieved by injecting DNA samples into the separation chamber, as illustrated in Figure 1 b. The applied pulsed potentials generated asymmetric obtuse-angle pulsed fields across the separation chamber, where the angle between the pulsed fields is ca. 135° and $E_1 = 1.4\,E_2$ in all experiments. Within the separation chamber, different sizes of DNA separate from each other and form individual streams, each stream deflecting an angle θ from the injection angle, as shown in Figure 1 c.

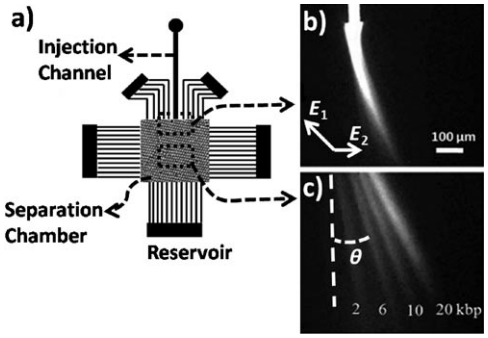

Figure 1. a) Schematic and b,c) photomicrographs of the DNA separation microchip used in this work. DNA solution is injected continuously into the separation chamber. White arrows represent the directions of the applied electric fields (b). The separation chamber is filled with nanoparticle arrays. Different sizes of DNA molecules separate from each other and form individual streams, each deflecting an angle θ from the injection angle (c).

It was observed that θ was highly dependent on the frequency, electric field strength, and DNA size. We have developed a geometric model that links these operating parameters to molecular size and separation angle, θ. A geometric model was first introduced by Austin et al.[8] to quantify one-dimensional zone electrophoretic separation of DNA within a microfabricated array structure under a pulsed field. Their attempt to fit the model to their observations required a coiling factor,[8,9] accounting for incomplete stretching of DNA. Here, a similar geometric model was developed for continuous two-dimensional angular separation of DNA under a pulsed field. We have assumed fully stretched DNA, so no fitting coefficient is utilized. The model is based on the known separation mechanism of DNA molecules under asymmetric obtuse-angle pulse fields.[6–8] According to this model, DNA reptates along the direction of the electric field as a flexible rod with a constant length (L). Once the direction of the electric field is changed, the molecule backtracks to a new direction as shown in Figure 2 a–c.

For small frequencies, when the molecule has enough time to reorient itself to the new direction and travel distances larger than its own length, a simple geometric equation can be derived. The model relates the net angular distance that the molecule travels at the end of one cycle (deflection angle, θ) to the molecular size (L), electric fields (E_1, E_2), and frequency (f):

[*] Prof. D. J. Harrison
Department of Chemistry, University of Alberta
Edmonton AB, T6G 2G2 (Canada)
Fax: (+1) 780-492-8231
E-mail: jed.harrison@ualberta.ca
Homepage: http://www.chem.ualberta.ca/faculty_staff/faculty/harrison.html
N. Nazemifard, Prof. S. Bhattacharjee
Department of Mechanical Engineering, University of Alberta
Edmonton AB, T6G 2G8 (Canada)
Prof. J. H. Masliyah
Department of Chemical Engineering, University of Alberta
Edmonton AB, T6G 2V4 (Canada)

[**] This work was supported by the Natural Sciences and Engineering Research Council of Canada (NSERC) and Alberta Ingenuity Fund. Microfabrication in this work was done at Nanofab, University of Alberta.

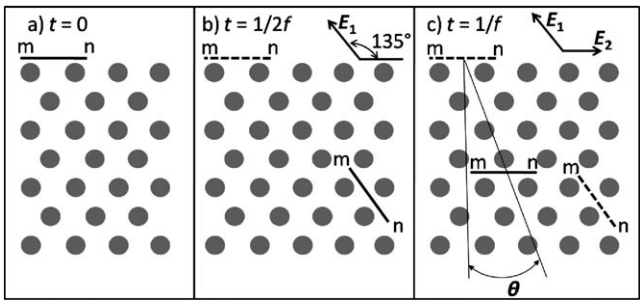

Figure 2. Geometric model for angular separation of DNA molecules during one cycle of electric pulses; m and n label the ends of the DNA molecule. a) Initial position of the molecule at the beginning of the cycle. b) Position of the molecule at the end of half cycle. c) Position of the molecule at the end of one cycle.

$$\tan\theta = 1-\sqrt{2}\left(\frac{\mu_2 E_2}{2f}-L\right)\Big/\left(\frac{\sqrt{2}\mu_1 E_2}{2f}-L\right) \quad (1)$$

where μ_1 and μ_2 are DNA mobilities along E_1 and E_2, respectively. According to Equation (1), when the frequency is very small, $\tan\theta = 1-(\mu_2/\mu_1)$, implying that θ is independent of DNA size. On the other hand, when the frequency increases up to a value of $f = (\mu_2 E_2)/(2L)$, $\tan\theta = 1$, giving a θ value of 45°. Here, the net DNA displacement only occurs along the stronger field E_1, since DNA cannot reorient completely along E_2 and θ reaches its maximum value of 45° independent of DNA size. According to this simple model, further increase in the frequency will result in trapping of DNA around a hook, since the DNA cannot align itself completely with either field vector. The model does not include a tortuosity factor, however, the use of experimentally determined mobility values (see below) should compensate for this.

The geometric model assumes DNA migrates along the direction of the electric field, leading with a head. In Figure 2a,b, n marks the head of the DNA, whilst in Figure 2c, m marks the head. This approach follows the biased reptation model developed by Zimm et al.[10] and Slater et al.[11] According to their model, when an electric field is applied to DNA in a confinement smaller than its gyration radius, migration occurs by one of two mechanisms: 1) a sliding motion in the direction of the electric field led by one of the heads, which was termed reptation by de Gennes;[12] or 2) creation of loops or hernias in the middle of the DNA chain. According to the biased reptation model, the formation of hernias would be improbable as long as external forces applied on the DNA chain are smaller than thermal forces.[13,14] Viovy et al.[1] introduced a scaled electric force parameter ε, which is the ratio of the electrostatic force to the thermal force applied on a DNA chain:

$$\varepsilon = \frac{\eta d_p^2 \mu_0 E}{kT} \quad (2)$$

where η is the buffer viscosity, μ_0 is DNA mobility in free solution, k is the Boltzmann constant, and T is the absolute temperature. According to the biased reptation model, when $\varepsilon \ll 1$, hernia formation and therefore DNA length fluctuations are at a minimum inside the pores, whereas they become significant for $\varepsilon \geq 1$. The value of ε in our experiments was calculated by substituting the experimental parameters used, with $\eta = 10^{-3}\,\mathrm{m^2 s^{-1}}$, $\mu_0 = 3.5\times10^{-8}\,\mathrm{m^2 V^{-1} s^{-1}}$, $E = 28000\,\mathrm{V m^{-1}}$, giving $\varepsilon = 0.05$, 0.60, and 2.61 for $d_p = 15$, 50, and 105 nm, respectively. Thus, the probability of hernia formation in the larger pore sizes is not negligible, while it should be negligible for 15 nm pores.

A key assumption in developing the geometric model was that DNA size fluctuation is negligible and the length is the contour length of the molecule. The effect of confinement on DNA stretching or elongation has been studied.[3,15–19] Tegenfeldt et al.[15] and Reisner et al.[19] provided empirical equations that relate the ratio of L/L_{contour} to the confinement size, stating:

$$\frac{L}{L_{\mathrm{contour}}} = \left(\frac{l_p w}{D^2}\right)^{1/3} \quad D \geq l_p \quad (3a)$$

$$\frac{L}{L_{\mathrm{contour}}} = 1 - 0.361\left(\frac{l_p}{D}\right)^{2/3} \quad D \ll l_p \quad (3b)$$

where l_p is the persistence length of DNA (ca. 50 nm), w is the molecule width (ca. 2 nm for double stranded DNA), and D is the confinement size. Stretching of DNA is assumed to be due to self-exclusion and the interplay of confinement and intrinsic elasticity of DNA, when no external electric force is applied. Substituting the pore sizes used in our experiments as D in this equation, L/L_{contour} was calculated for each pore size, giving 0.84, 0.34, and 0.21 for $l_p = 15$, 50, and 105 nm, respectively. These results cannot be used in our study to estimate the length of DNA inside the nanoparticle array, since our experiments were conducted under strong electric fields which further stretch DNA molecules. However, according to Equation (3), mere confinement in pore sizes around 15 nm is sufficient to stretch DNA molecules up to 84% of their contour length. If the additional stretching of DNA under high electric field is considered too, it is obvious that the assumption of fully stretched DNA employed in developing the geometric ratchet model is valid for pore sizes of 15 nm or less.

A comparison between the predicted DNA deflection angle [Eq. (1)] and those obtained experimentally provides insight into the migration mechanism of DNA molecules in pore sizes ranging around the DNA persistence length (ca. 50 nm). In order to calculate the DNA deflection angle θ, predicted by Equation (1), the mobility μ of DNA was determined. For 20 kbp DNA migrating through 15 nm pores under $280\,\mathrm{V cm^{-1}}$, the mobility was $\mu = (3.88\pm0.62)\times10^{-5}\,\mathrm{cm^2 V^{-1} s^{-1}}$. In calculating Equation (1), the molecule length L was assumed to be the contour length of the molecule, $L = L_{\mathrm{contour}}$. The results are shown in Figure 3, which plots the variation of deflection angle θ for 20 kbp DNA molecules with respect to frequency. The solid line represents θ calculated by Equation (1) while experimental results are shown by symbols. The experiment was conducted for three different pore sizes, 15, 50, and 105 nm. Figure 3 shows that the geometric model has the best agreement with experimentally obtained values of θ for a 15 nm pore size, while the

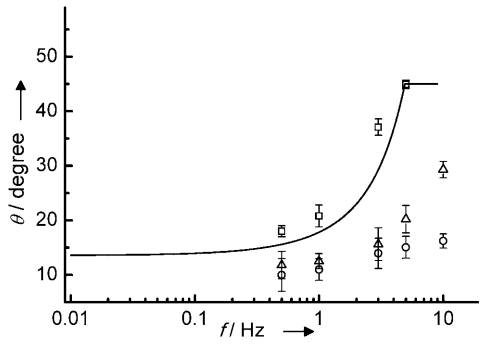

Figure 3. Variation of deflection angle θ of 20 kbp DNA with respect to frequency f. Solid line (——) represents the prediction of geometric model [Eq. (1)]. Symbols represent the experimentally obtained deflection angles of 20 kbp DNA in three different pore sizes (d_p); □: 15 nm, △: 50 nm, ○: 105 nm. $E_1 = 280\ \mathrm{V\,cm^{-1}}$.

observed θ for larger pore sizes do not match the predictions. This behaviour was further investigated for other DNA sizes (48 kbp and 166 kbp) and similar behaviour was observed.

As stated earlier, the simple geometric model predicts a rising curve for DNA deflection angle that reaches a maximum of 45° with increasing frequency, independent of DNA size. Figure 4 shows the experimentally observed

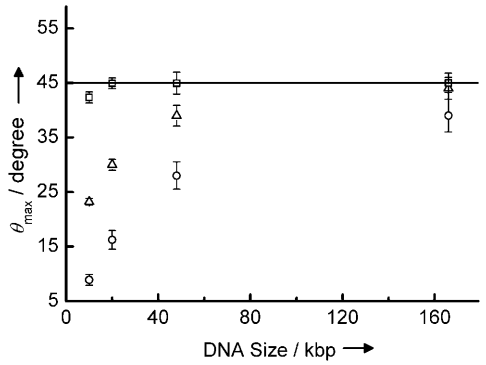

Figure 4. Effects of DNA size on maximum deflection angle, θ_{max}. Solid line represents prediction of geometric model as, $\theta_{max} = 45°$, independent of DNA size. Symbols represent experimental values of θ_{max} for three different pore sizes (d_p); □: 15 nm, △: 50 nm, ○: 105 nm. $E_1 = 280\ \mathrm{V\,cm^{-1}}$.

maximum deflection angle, θ_{max}, corresponding to different DNA sizes ranging from 10 to 166 kbp, in pore sizes ranging from 15 to 105 nm, at an electric field of $E_1 = 280\ \mathrm{V\,cm^{-1}}$. The frequencies were varied in each study, to determine θ_{max}. It can be seen from Figure 4 that for pore sizes of 50 nm and 105 nm, the maximum deflection angle θ_{max} is strongly dependent on DNA size, contrary to the prediction of the geometric model. We conclude that molecular dynamics of DNA electrophoresis such as size fluctuation and hernia formation significantly affect the deflection behaviour in larger pore sizes. However, for a pore size of 15 nm, θ_{max} is around 45° regardless of DNA size, as predicted by the geometric model.

Our results in Figure 3 and 4 show that a pore size of 15 nm, which is smaller than the persistence length of DNA and gives $\varepsilon = 0.05$ under our conditions, allows a quantitative fit of the geometric model to the experimental observations when full stretching is assumed. The larger pore sizes do not sufficiently confine DNA and do not prevent the formation of hernias, resulting in the deviation of deflection behaviour of a molecule from the geometric models.

One of the advantages of having an analytical expression to predict the deflection behaviour of DNA is that the effect of different experimental parameters on the separation efficiency can be known a priori. It has been shown experimentally that the effect of field and frequency on DNA separation resolution are coupled.[5,20,21] Presently, many exploratory experiments are required to determine the best conditions for resolving different DNA sizes. Figure 5a shows the variation of θ with respect to f for

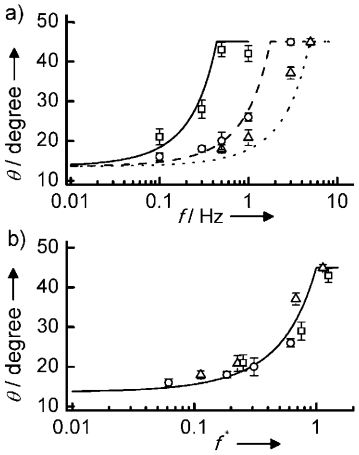

Figure 5. a) Frequency dependent behavior of deflection angles of different sizes of DNA molecules (20, 48, 166 kbp) in $d_p = 15$ nm pores ($\mu = 3.88$, 3.42, and $2.29 \times 10^{-5}\ \mathrm{cm^2\,V^{-1}\,s^{-1}}$, correspondingly). $E_1 = 280\ \mathrm{V\,cm^{-1}}$. Lines represent θ predicted by the geometric model [Eq. (1)] where symbols are the experimental results for θ. △ and -----: 20 kbp, ○ and – – –: 48 kbp, □ and ——: 166 kbp. b) Variation of θ with respect to scaled frequency, f^*, for the data set shown in (a). △: 20 kbp, ○: 48 kbp, □: 166 kbp, ——: geometric model [Eq. (6)].

three different DNA sizes; 20, 48, and 166 kbp in 15 nm pores. The solid lines represent θ predicted by the geometric model [Eq. (1)] whereas the symbols represent θ obtained experimentally in 15 nm pores with an electric field of $E_1 = 280\ \mathrm{V\,cm^{-1}}$. We have found that by manipulating Equation (1) and employing the reorientation time of DNA, it is possible to normalize these results to provide a predictive model to establish optimal separation conditions. Equation (1) can be manipulated to yield:

$$\tan\theta = 1 - \frac{\mu_2}{\mu_1}\left(1 - \frac{2fL}{\mu_2 E_2}\right) \Big/ \left(1 - \frac{\sqrt{2}\mu_2}{\mu_1}\left(\frac{2fL}{\mu_2 E_2}\right)\right) \qquad (4)$$

where μ_2/μ_1 can be determined from independent mobility measurement (1.32 in our experiment for $d_p = 15$ nm). The term $L/(\mu_2 E_2)$ is the time for the molecule to travel its own

length under the applied electric field (reorientation time of DNA) and $1/(2f)$ is the pulse time. Hence, the ratio of these two parameters is a dimensionless number which can be considered as the scaled frequency, f^*

$$f^* = f/\left(\frac{\mu_2 E_2}{2L}\right) \tag{5}$$

Making use of Equation (5), Equation (4) becomes:

$$\tan\theta = 1-\frac{\mu_2}{\mu_1}(1-f^*)/\left(1-\frac{\sqrt{2}\mu_2}{\mu_1}f^*\right) \tag{6}$$

The variation of θ with respect to f^* predicted by Equation (6) is shown in Figure 5b; the three solid lines of Figure 5a have merged into one line by non-dimensionalizing Equation (1). Figure 5b shows that in pore sizes smaller than the persistence length of DNA, the frequency response for different sizes of DNA can be normalized to one effective response curve, using the reorientation time of the DNA, which is a size dependent parameter. This result shows that the effects of electric field, frequency, and DNA size on the separation efficiency of DNA molecules can be integrally linked in one defining parameter. For instance, according to the definition of f^* [Eq. (5)], if the electric field is increased, in order to preserve the same separation efficiency, the pulse frequency should be increased as well.

Several authors[22–24] predicted that the migration of DNA in the regime where pore sizes are smaller than the persistence length of DNA, follows the biased reptation mechanism. DNA separation experiments in tight gels supported their predictions. Based on their predictions, we developed a simple geometric model which has a quantitative agreement with our experiments in fabricated, ordered, porous media. Our results show that when the confinement scales are smaller than the persistence length of DNA, the bending elasticity of the molecule prevents formation of hernias and the molecule can be treated as a persistent chain. This allows the use of much simpler deterministic models for simulating DNA dynamics in nanoscale confinement. In contrast, DNA migration through larger pores involves complicated conformations of the molecule such as hernia formation and significant size fluctuation, which necessitate a more sophisticated numerical simulation to model the deflection behaviour of DNA molecules. The present study shows that small ordered confinements achieved by the colloidal self-assembly (CSA) approach can provide a reliable tool to study the dynamic behaviour of DNA and to validate the existing theoretical models such as the reptation model or "lakes-straits" model of Zimm.[26] We have shown that greater confinement, allowed by the CSA fabrication method, leads to fully stretched DNA and more efficient separation of DNA.

Received: November 10, 2009
Published online: March 15, 2010

Keywords: DNA · microfluidics · nanopores · pulsed field electrophoresis · self-assembly

[1] J. L. Viovy, *Rev. Mod. Phys.* **2000**, *72*, 813–872.
[2] R. Austin, *Nat. Mater.* **2003**, *2*, 567–568.
[3] T. J. Odijk, *J. Chem. Phys.* **2006**, *125*, 204904.
[4] Y. Zeng, D. J. Harrison, *Anal. Chem.* **2007**, *79*, 2289–2295.
[5] Y. Zeng, M. He, D. J. Harrison, *Angew. Chem.* **2008**, *120*, 6488–6491; *Angew. Chem. Int. Ed.* **2008**, *47*, 6388–6391.
[6] C. Bustamante, S. Gurrieri, S. B. Smith, *Trends Biotechnol.* **1993**, *11*, 23–30.
[7] S. Gurrieri, S. B. Smith, K. S. Wells, I. D. Johnson, C. Bustamante, *Nucleic Acids Res.* **1996**, *24*, 4759–4767.
[8] T. A. J. Duke, R. H. Austin, E. C. Cox, S. S. Chan, *Electrophoresis* **1996**, *17*, 1075–1079.
[9] L. R. Huang, J. O. Tegenfeldt, J. J. Kraeft, J. C. Sturm, R. H. Austin, E. C. Cox, *Nat. Biotechnol.* **2002**, *20*, 1048–1051.
[10] O. J. Lumpkin, P. Dejardin, B. H. Zimm, *Biopolymers* **1985**, *24*, 1573–1593.
[11] G. W. Slater, J. Noolandi, *Biopolymers* **1985**, *24*, 2181–2184.
[12] P. G. de Gennes, *J. Chem. Phys.* **1971**, *55*, 572.
[13] B. Åkerman, *Prog. Biophys. Mol. Biol.* **1996**, *65*, PB144–PB144.
[14] B. Åkerman, *Phys. Rev. E* **1996**, *54*, 6697–6707.
[15] J. O. Tegenfeldt, C. Prinz, H. Cao, S. Chou, W. W. Reisner, R. Riehn, Y. M. Wang, E. C. Cox, J. C. Sturm, P. Silberzan, R. H. Austin, *Proc. Natl. Acad. Sci. USA* **2004**, *101*, 10979–10983.
[16] J. O. Tegenfeldt, H. Cao, W. W. Reisner, C. Prinz, R. H. Austin, S. Y. Chou, E. C. Cox, J. C. Sturm, *Biophys. J.* **2004**, 596A–596A.
[17] T. Odijk, *Phys. Rev. E* **2008**, *77*, 060901.
[18] R. M. Jendrejack, D. C. Schwartz, M. D. Graham, J. J. de Pablo, *J. Chem. Phys.* **2003**, *119*, 1165–1173.
[19] W. Reisner, K. J. Morton, R. Riehn, Y. M. Wang, Z. N. Yu, M. Rosen, J. C. Sturm, S. Y. Chou, E. Frey, R. H. Austin, *Phys. Rev. Lett.* **2005**, *94*, 196101.
[20] L. R. Huang, P. Silberzan, J. O. Tegenfeldt, E. C. Cox, J. C. Sturm, R. H. Austin, H. Craighead, *Phys. Rev. Lett.* **2002**, *89*, 178301.
[21] J. Han, H. G. Craighead, *Science* **2000**, *288*, 1026–1029.
[22] A. N. Semenov, T. A. J. Duke, J. L. Viovy, *Phys. Rev. E* **1995**, *51*, 1520–1537.
[23] C. Heller, C. Pakleza, J. L. Viovy, *Electrophoresis* **1995**, *16*, 1423–1428.
[24] T. A. J. Duke, J. L. Viovy, *Phys. Rev. Lett.* **1992**, *68*, 542–545.
[25] H. Zhang, M. J. Wirth, *Anal. Chem.* **2005**, *77*, 1237–1242.
[26] B. H. Zimm, *J. Chem. Phys.* **1991**, *94*, 2187–2206.

